Expert Systems
The Journal of Knowledge Engineering

Article

DOI: 10.1111/j.1468-0394.2009.00479.x

An automated hierarchical gait pattern identification tool employing cross-correlation-based feature extraction and recurrent neural network based classification

Saibal Dutta,[1] Amitava Chatterjee[2] and Sugata Munshi[2]

(1) Heritage Institute of Technology, Electrical Engineering Department, Kolkata, India, PIN 700107

(2) Jadavpur University, Electrical Engineering Department, Kolkata, India, PIN 700 032

Email: cha_ami@yahoo.co.in

Abstract: *In this paper Elman's recurrent neural network (ERNN) is employed for automatic identification of healthy and pathological gait and subsequent diagnosis of the neurological disorder in pathological gaits from the respective gait patterns. Stance, swing and double support intervals (expressed as percentages of stride) of 63 subjects were analysed for a period of approximately 300 s. The relevant gait features are extracted from cross-correlograms of these signals with corresponding signals of a reference subject. These gait features are used to train modular ERNNs performing binary and tertiary classifications. The average accuracy of binary classifiers is obtained as 90.6%–97.8% and that of tertiary classifiers is 89.8%. Hence, two hierarchical schemes are developed each of which uses more than one modular ERNN to segregate healthy, Parkinson's disease, Huntington's disease and amyotrophic lateral sclerosis subjects. The average testing performances of the schemes are 83.8% and 87.1%.*

Keywords: gait analysis, feature extraction, cross-correlation, modular recurrent neural networks, hierarchical classifiers

1. Introduction

Walking is a complicated mechanical action which is very important for normal functioning of human beings. The process is automatically controlled by the nervous system and some abnormalities in the nervous system may cause uncontrolled and improper movements. An automated gait pattern identification tool that can differentiate between healthy and pathological subjects and can identify the disease causing the neurological disorder can be very useful in real life to recognize gait degeneration and suggest proper course of treatment. This can also help to prevent falls which can potentially avoid several catastrophic situations. Hence gait signal analysis has become an important area of research from the early 1990s (Davis, 1988; Winter, 1991; Fildes, 1994; Nigg *et al*., 1994).

Several researchers have employed different ways of analysing gait signals. Most of these schemes explore several types of signal acquisition procedures by acquiring signals from several parts of the human anatomy that are

directly related to gait and posture, and then adopting several procedures for extracting meaningful features from the acquired signals. Many of these methodologies are based on the recording of (Davis, 1988)

- step frequency or cadence
- step length or length of one step
- stride length or distance between two steps
- stride interval (stance, swing and double support interval)
- reaction force or force exerted by a person on the floor while walking
- orthopaedic angles or orientation of limb segments
- electromyographic activity of the involved musculature during walking
- minimum foot clearance during walking, during the mid swing phase of the gait cycle

While many of the schemes proposed so far address the issue of segregating gait signals into young and old categories (Winter, 1991; Nigg *et al*., 1994; Ostrosky *et al*., 1994; Begg *et al*., 2005), not much work has been reported on the determination of neurological diseases and segregating subjects from healthy human beings on the basis of gait signal analysis (Holzreiter & Kohle, 1993; Carletti *et al*., 2006). While young–elderly classification of gait signals is very important to identify at-risk gait in the older population at an early stage, to take preventive measures against fall (Begg *et al*., 2005), automatic determination of whether a subject is suffering from a neurological disease and, if yes, from which type of neurological disease is also very important to prescribe further course of therapy. In fact, compared to a young–elderly classification scheme, a disease identification scheme should be considered a more complex problem because the former scheme requires the performance of a binary classification job (i.e. a two-class classification) and the latter problem requires the performance of a multi-class classification job with more than two classes.

The present paper proposes the development of an automated gait identification tool which can automatically classify whether the subject under consideration is a healthy one and, if not, whether the source of neurological disorder in the pathological subject is due to Parkinson's disease (PD), Huntington's disease (HD) or amyotrophic lateral sclerosis (ALS). The overall purpose of the proposed method is to predict whether an unknown subject under consideration is healthy or suffering from one of the three major neurological diseases. This is achieved by developing a classifier which can analyse gait signals from the subject under consideration to predict in which class the subject belongs, i.e. the class of healthy people, the class of people suffering from PD, the class of people suffering from HD or the class of people suffering from ALS. The determination of a suitable solution for the problem is based on decomposing the problem into two subproblems:

(a) the determination of a suitable method for meaningful feature extraction from gait signals and
(b) designing a suitable classification algorithm based on those features extracted.

For the problem under consideration, for each subject several gait parameters are considered, namely the stance interval, the swing interval and the double support interval, all expressed as percentages of stride time. As stance, swing and double support intervals associated with walking tend to be different for normal and pathological subjects, features derived from them can potentially be useful to develop healthy and pathological classification models. The consecutive stance intervals, swing intervals and double support intervals are considered to constitute three separate time series (sequences) or discrete-time signals. For each such signal acquired from each subject, the feature extraction is carried out by determining the signal's cross-correlogram with a reference subject's corresponding signal and then extracting some relevant features from each such cross-correlogram. This is followed by the development of a supervised network for classification, utilizing the features extracted as inputs. For our system, we propose Elman's recurrent neural network (ERNN) (Bose & Liang, 1998; Haykin, 2004) to perform this classification. In general, several neural network based methodologies have been proposed in the literature for biomedical

signal processing and decision support systems (Pizzi, 2001; Güler & Übeyli, 2005, 2006; Barişçi & Hardalaç, 2007; Durbin *et al.*, 2008). ERNNs have also been previously employed for pattern recognition problems in other problem domains (Lee & Song, 1997). ERNNs are a special type of supervised neural networks which employ both feedforward and feedback connections to perform multidimensional mathematical mapping, and they are suitable for learning both temporal and spatial inputs. In this paper we propose two different schemes, each utilizing more than one modular ERNN in hierarchical form, which can be used as composite solution systems. The proposed schemes have been tested for several benchmark signals and the performance exhibited encouraging results compared to several fuzzy clustering methods and the backpropagation neural network (BPNN) based classifier.

The rest of the paper is organized as follows. Section 2 presents a brief description of the gait signals and their acquisition procedure. The cross-correlation technique based feature extraction methodology is detailed in Section 3. The ERNN based classification scheme and two composite schemes employing modular ERNNs in hierarchical fashion are presented in Section 4. Section 5 presents a performance evaluation. Conclusions are presented in Section 6.

2. Acquisition of gait signals

For the system under consideration, we have utilized benchmark gait signals that are freely available from the Physionet database.[1] The database contains real-life gait signals acquired from both healthy subjects and pathological subjects with neurological disorders due to PD, HD and ALS. This database maintains a measure of disease severity or duration, to indicate how severely a person (present in that database) is affected by PD, HD or ALS. The database uses the Hohn and Yahr score for subjects suffering from PD. A higher value of this score indicates a more advanced condition of the disease. The score varies from 1.5 to 4 for the PD subjects under consideration here. For 60% of these patients, the score is 3 or more, signifying a more advanced state of the disease. The database uses the total functional capacity measure for HD subjects. Here a lower score indicates more advanced functional impairment. The score varies from 1 to 12 for the HD subjects under consideration. Here, for almost 50% of these patients, the score is 5 or less (signifying a more severe state of the disease), and for the remaining 50% the score is more than 5. For the subjects suffering from ALS, the severity measure maintained by the database is the time since the onset of the disease. Here, for almost 80% of these ALS patients, the severity of the ALS disease is moderate.

The subjects were instructed to walk at their normal speed along a 77 m long hallway. To measure gait rhythm and the timing of gait cycle, force-sensitive insoles were placed in each subject's shoe. The gait time sequences were obtained using these force-sensitive resistors, with output roughly proportional to the force under the foot. Stride to stride measures of footfall contact times were derived from these signals, and the stride time (i.e. the time from initial contact of one foot to subsequent contact of the same foot) along with swing and stance times were determined for each stride. For each subject, stride to stride measurements of footfall contact times are acquired for approximately 300 s. In the present study, we have considered the time sequences corresponding to the left and right stance intervals, the left and right swing intervals and the double support interval, each expressed as a percentage of the stride time, for each subject. Figures 1–3 demonstrate the time sequence plots of the left swing interval, the right stance interval and the double support interval for some sample subjects. A close inspection of these plots reveals that it is impossible to differentiate between healthy and pathological subjects without any ambiguity. This indicates that the need for an automated system that can automatically classify pathological and healthy subjects is paramount.

To further strengthen this observation, we carried out frequency analyses of some sample signals from each class. Figure 4 shows the

[1] *http://physionet.fri.uni-lj.si/physiobank/database/gaitndd/. Last accessed 29 November 2007.*

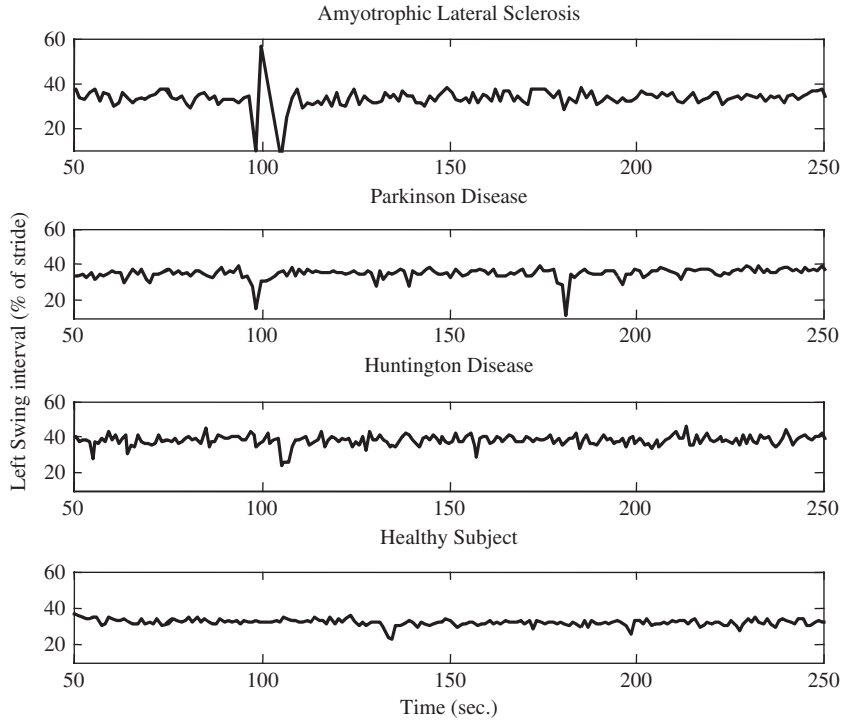

Figure 1: *Plot of left swing interval (% of stride) versus time for sample healthy and pathological subjects.*

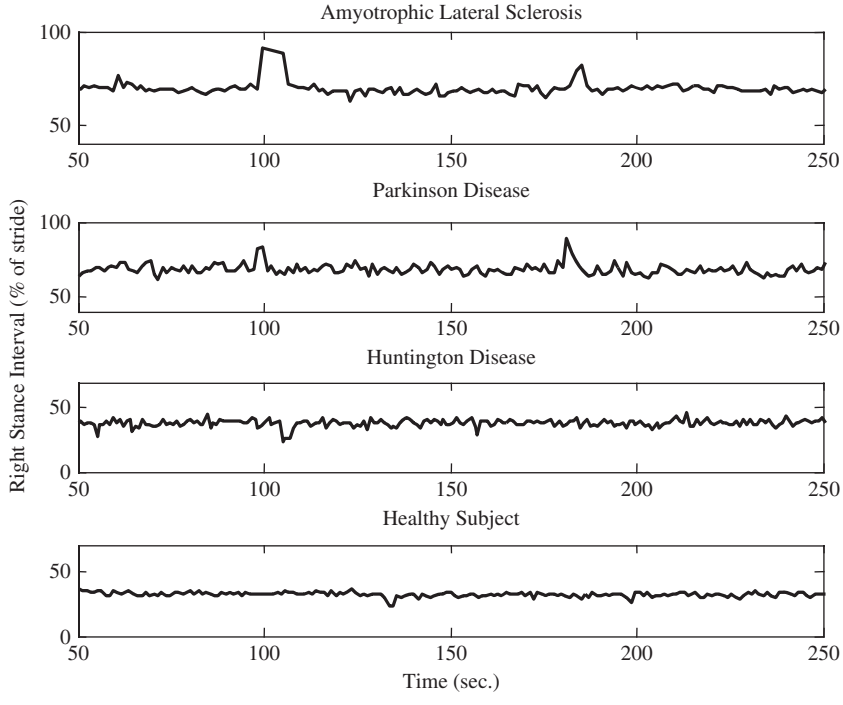

Figure 2: *Plot of right stance interval (% of stride) versus time for sample healthy and pathological subjects.*

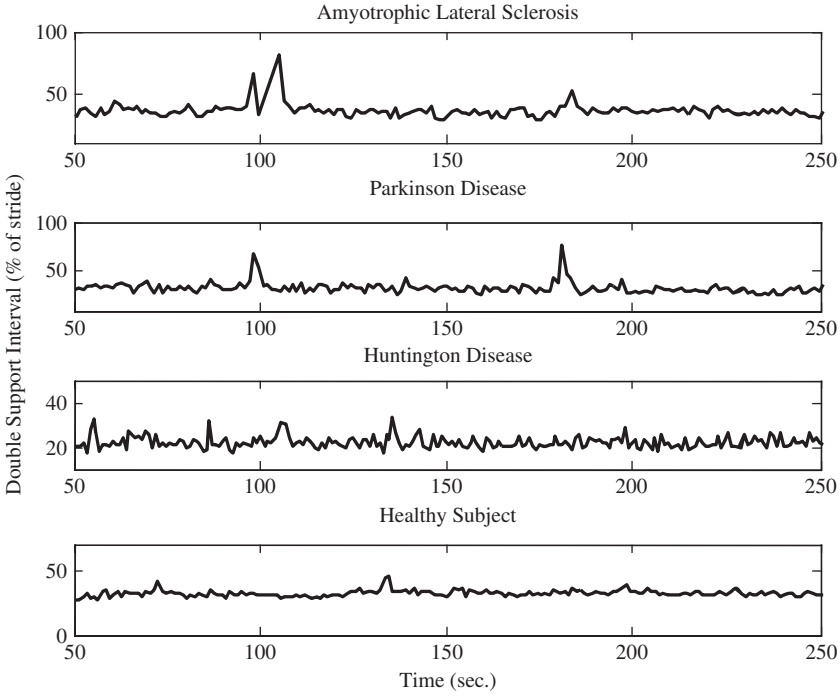

Figure 3: *Plot of double support interval (% of stride) versus time for sample healthy and pathological subjects.*

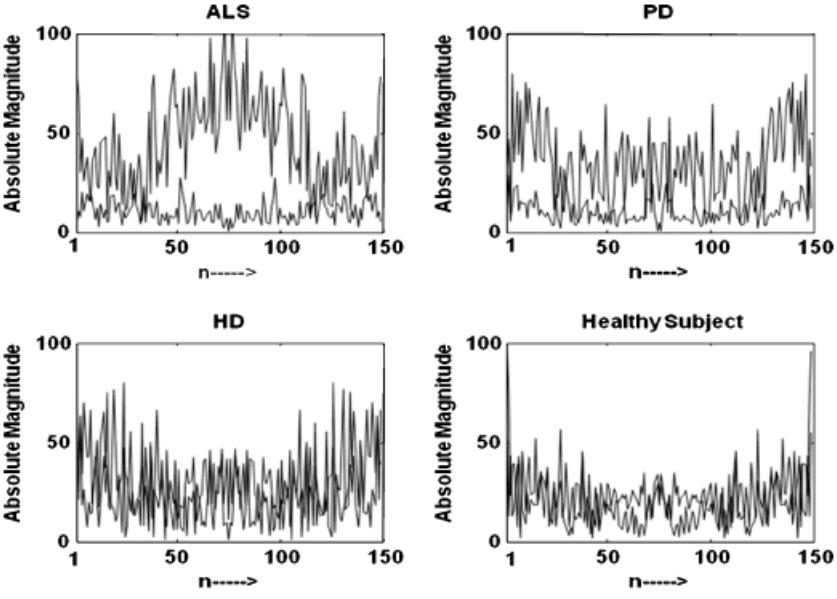

Figure 4: *Plot of the absolute magnitudes of the fast Fourier transform coefficients for the left stance interval signals of sample subjects belonging to different classes.*

results of these analyses, computed by employing fast Fourier transform, carried out for two left stance interval signals belonging to each class, i.e. the gait signals acquired for two sample healthy subjects, two sample subjects suffering from PD, two sample subjects suffering from HD and two sample subjects suffering from ALS. The figure shows plots of the absolute magnitudes of the discrete Fourier coefficients computed for each signal. These plots

also demonstrate that even computation of frequency analysis, utilizing Fourier transform, is not sufficient to clearly infer whether a signal belongs to a particular class or not.

3. Cross-correlation-based feature extraction

The mathematical technique of cross-correlation of two signals is aimed at answering the question: to what extent are the two signals correlated? In other words, it provides quantitative information about the extent to which a definite pattern of relationship exists between the signals.

The cross-correlation technique has been conveniently utilized in robotics and remote-sensing applications, for comparing different images. It has also been used in sonar and radar systems for range and position detection, in the recovery of signals buried in noise, and in several other domains (Ifeacher & Jervis, 2001; Roberts, 2003). A few papers employing the cross-correlation technique in the realm of biomedical signal processing have been reported in the literature (Suljagic *et al*., 1996; Kuppusamy *et al*., 1997; Mizuno-Matsumoto *et al*., 2002, 2005). However, one of the novelties of the present work lies in applying the cross-correlation technique judiciously, as a feature extraction tool, for the problem of gait signal processing.

The cross-correlation of two finite duration causal sequences $x[n]$ and $y[n]$, each of length N samples, is obtained as

$$r_{xy}[m] = \sum_{n=0}^{N-|m|-1} x[n]y[n-m] \qquad (1)$$

$$m = -(N-1), -(N-2), \ldots, 0, 1, 2, 3, \ldots, N-1$$

In this work, as mentioned earlier, one of the healthy subjects is chosen as reference. The stance interval (left and right), swing interval (left and right) and double support sequences of each of the other subjects are cross-correlated with the corresponding sequences of the reference. This yields five cross-correlograms for each subject. As equation (1) represents the formula for unbiased correlation, it should be kept in mind that the beginning and the end of a signal have important contributions in the cross-correlogram generated. Hence, in our experiments, these are kept uniform for all signals and each signal considered is of uniform length. Some representative sets of cross-correlograms are depicted in Figure 5. Here, a signal from the reference subject is $x[n]$ and the corresponding signal from any other subject is $y[n]$. Three traits of the cross-correlation sequences, expressed quantitatively by the centroid (*cent*), the mean-square abscissa (*msa*) and the variance of the abscissa (*va*) (Bracewell, 2000), are found to serve as important indicators of the neurological state of the subjects. They are defined as

$$cent = \langle m \rangle = \frac{\sum_{m=-(N-1)}^{N-1} m r_{xy}[m]}{\sum_{m=-(N-1)}^{N-1} r_{xy}[m]} \qquad (2)$$

$$msa = \langle m^2 \rangle = \frac{\sum_{m=-(N-1)}^{N-1} m^2 r_{xy}[m]}{\sum_{m=-(N-1)}^{N-1} r_{xy}[m]} \qquad (3)$$

$$va = \langle (m - \langle m \rangle)^2 \rangle = \frac{\sum_{m=-(N-1)}^{N-1} (m - \langle m \rangle)^2 r_{xy}[m]}{\sum_{m=-(N-1)}^{N-1} r_{xy}[m]} \qquad (4)$$

The above quantitative descriptors of the cross-correlograms are evaluated for several subjects with known neurological states of health and these values are subsequently used to train the recurrent neural networks (RNNs). Once this process is complete, it is expected that for a new subject, if the above quantities are calculated and fed to the RNNs, the system can determine whether the subject is healthy or not, and also the type of illness, where the subject is found to be ill. The three features extracted from the left stance interval sequence of a subject

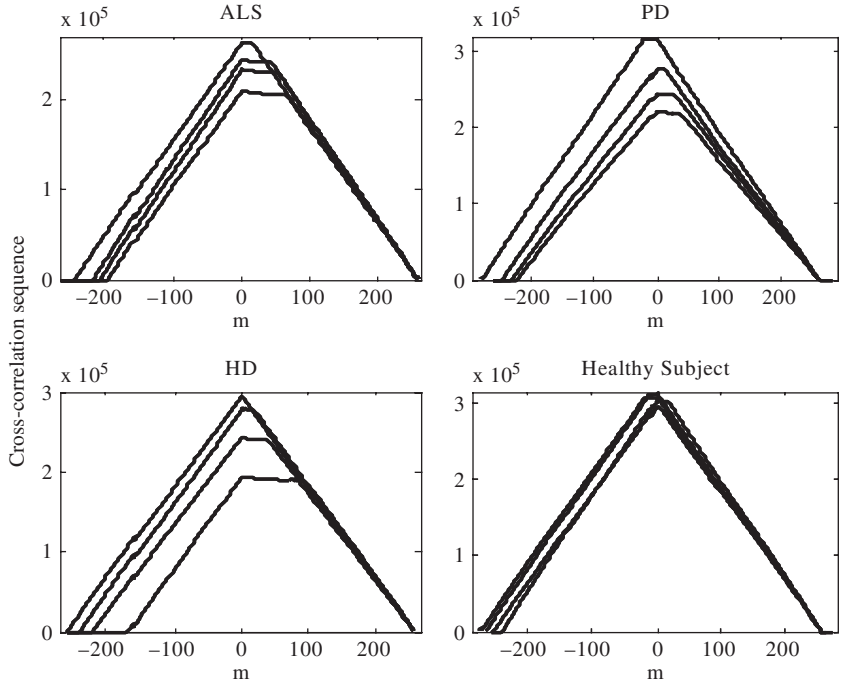

Figure 5: *Representative cross-correlograms of the left stance interval sequences for subjects belonging to different classes.*

are named as *cent_l_st*, *msa_l_st* and *va_l_st*. Similarly the three features extracted from the right stance interval sequence are named as *cent_r_st*, *msa_r_st* and *va_r_st*, the three features extracted from the left swing interval sequence are named as *cent_l_sw*, *msa_l_sw* and *va_l_sw*, the three features extracted from the right swing interval sequence are named as *cent_r_sw*, *msa_r_sw* and *va_r_lw*, and the three features extracted from the double support sequence are named as *cent_ds*, *msa_ds* and *va_ds*. Hence, for each subject under consideration, 15 features are extracted from five cross-correlograms. Table 1 presents a list of these features, used as the inputs for each RNN, with their range of values obtained for our specific problem under consideration.

4. ERNN based hierarchical classification tool

4.1. ERNNs

RNNs are especially useful for learning both temporal and spatial patterns. Compared with a multilayer perceptron (MLP), which employs only feedforward connection, RNNs are more complicated as they employ a combination of feedback and feedforward connections, exhibiting the property of memory (Bose & Liang, 1998; Haykin, 2004). RNNs are useful for two types of application: as associated memories and for input–output mapping (Zhou & Xu, 1999; Delgado *et al.*, 2006; Süt & Şenocak, 2007; Übeyli, 2007). In our application, we are interested in input–output mapping and there are several architecture layouts available for different relevant RNNs. Some popular variants of such RNNs include Jordan's network (which employs feedback connection from the output of the output layer to the input of the input layer) (Jordon, 1986), Elman's network (which employs feedback connection from the output of the hidden layer to the input of the input layer) (Lee & Song, 1997), the Pollack sequential cascade network (Pollack, 1991), the higher order RNN of Giles *et al.* (1990), Lee and Song's network (in which each output node is connected to itself) (Lee & Song, 1997) etc. In our system we have employed Elman's RNN, a

Table 1: *The range or universe of discourse for the selected features*

Features	*Range or discourse*
cent_l_st	[− 60, 35]
msa_l_st	[8524, 14100]
va_l_st	[6130, 12878]
cent_r_st	[− 59, 35]
msa_r_st	[8500, 14500]
va_r_st	[6122, 12900]
cent_l_sw	[− 60, 35]
msa_l_sw	[8442, 14000]
va_r_st	[6052,12829]
cent_r_sw	[− 60, 35]
msa_r_sw	[8440, 14040]
va_r_sw	[6050, 12830]
cent_ds	[− 59, 35]
msa_ds	[7574, 13920]
va_ds	[5990, 12745]

popular RNN in the category of dynamically driven neural networks. Like several other RNNs, Elman's network incorporates a static MLP architecture as its basic building block and employs some popular learning algorithms, employed for training MLPs, for their training. Figure 6 shows the generic architecture of an ERNN utilized in our work. This is a three-layer architecture where layer 2 contains context units in addition to the hidden neurons. The context units comprise a bank of unit time delay; they store the outputs of the hidden neurons for one time step and then these are fed back to the input of the input layer. Hence the context units depict the short-term memory of the RNN. However, as the output of the hidden layer of the RNN, at any time step, is a nonlinear function of both the output of the input layer at that given time step and the output of the hidden layer in the previous time step, the network continues to recycle information over multiple time steps, which is useful for efficient discovery of temporal patterns (Haykin, 2004). Mathematically speaking, the output from the hidden layer at the kth time step is given as

$$z_j^2(k) = f_1\left[\sum_{i=1}^{N} z_i^1(k) w_{ij}^{12} + \sum_{j=1}^{P} z_j^2(k-1) c_{jj}^{22} + b_j^2\right] \tag{5}$$

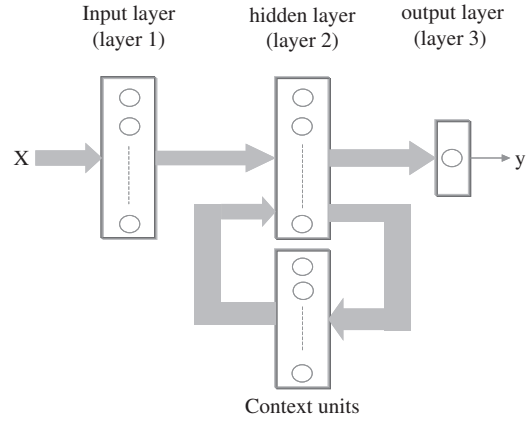

Figure 6: *The architecture of the ERNN.*

where $z_j^2(k)$ is the output of the jth neuron of layer 2 at the kth time step, $z_i^1(k)$ is the output of the ith neuron of layer 1 at the kth time step $x_i(k)$, w_{ij}^{12} is the weight connecting the ith neuron of layer 1 and the jth neuron of layer 2, c_{jj}^{22} is the weight connecting the jth neuron of context units and the jth hidden layer neuron of layer 2, $z_j^2(k-1)$ is the output of the jth neuron of layer 2 delayed by one time step, b_j^2 is the bias associated with the jth neuron of layer 2, N is the number of inputs and P is the number of hidden layer neurons. Hence the output of the ERNN can be given as

$$z^3(k) = f_2\left[\sum_{j=1}^{P} z_j^2(k) w_j^{23}\right] \tag{6}$$

where $z^3(k)$ is the output of the only neuron in the output layer at time step k, w_j^{23} is the weight connecting the jth neuron of layer 2 to the only neuron in layer 3, and $f_1(\bullet)$ represents a nonlinear function, usually chosen as a tan sigmoidal or log sigmoidal function. $f_2(\bullet)$ can be either a linear or a nonlinear mapping.

A generalized ERNN can employ multiple neurons in the output layer also. In the training phase, for a multiclass problem, the output, for each exemplar input to an ERNN, is chosen for our system as $y \in \{1, 2, \ldots, c, \ldots, C\}$. Here C is the total number of classes in which each RNN is designated to classify its inputs. In the implementation phase, the output of the ERNN

is classified as

$$y_{\text{class}} = c \quad \text{if } c - 0.5 < y \leq c + 0.5 \qquad (7)$$

except for the two terminal classes where $y_{\text{class}} = 1$ if $y < 1.5$ and $y_{\text{class}} = C$ if $y > C - 0.5$.

4.2. Hierarchical structure of modular ERNNs

The proposed system is configured as a four-class classification system (i.e. $C = 4$) where the four classes correspond to healthy subjects, pathological subjects suffering from PD, pathological subjects suffering from HD and pathological subjects suffering from ALS. Hence two schemes are proposed in this paper for solving the composite problem, where each scheme utilizes more than one ERNN in modular form. Each modular ERNN is designed to solve a subproblem and these ERNNs are arranged in a hierarchical fashion where the output of one ERNN determines whether another (or more than one) ERNN should be activated or not. Each ERNN is activated as a 15-input one-output system where the 15 inputs are determined from the features extracted from cross-correlograms, as discussed in Section 3.

For the proposed scheme 1, ERNN1 is trained to solve a binary classification problem where we determine whether the subject under test is healthy/pathological. If the subject is diagnosed to be pathological, then ERNN2 is activated with the same set of feature vectors, determined for that specific subject. ERNN2 is specifically trained with the training data set determined from pathological subjects only and it is designed to solve a three-class problem, segregating pathological subjects into PD, HD and ALS classes. Figure 7 shows the proposed scheme 1 in flowchart form. Finally, outputs from both ERNN1 and ERNN2 are utilized to suggest the ultimate diagnosis which classifies the subject under consideration into one of the four classes, i.e. healthy, PD, HD, ALS.

The same problem can also be solved by employing proposed scheme 2, shown in flowchart form in Figure 8. The feature extraction part remains identical to that of scheme 1 but the classification module now employs three modular ERNNs, namely ERNN1, ERNN3 and ERNN4, each trained to perform specific binary classification jobs. The ERNN1 implemented is identical to that proposed for scheme 1. But, if it diagnoses the subject as pathological, then ERNN3 is activated to determine whether the pathological subject is suffering from ALS or not. If the answer is negative, then ERNN4 is activated to determine whether the subject is suffering from PD or HD. The final outcome of the automated tool proposed in scheme 2 is determined by considering outputs from all three ERNNs.

5. Performance evaluation

To evaluate the performance of the proposed schemes we have considered the signals available (see footnote 1). As discussed earlier, we considered five time sequence gait signals for each subject. By constructing the corresponding cross-correlograms with reference to the corresponding signals acquired from the reference subject, we computed a total of 15 features for each subject (extracting three features from each of the five cross-correlograms). Table 1 shows the universe of discourse for all these features extracted from the entire signal database.

Once the feature extraction phase is over, each of the four modular ERNNs is trained based on their corresponding training data sets. The composite training and testing data sets are created by using 50% of the data in each data set. ERNN1 is trained utilizing the entire training data set, ERNN2 and ERNN3 are trained utilizing those exemplars in the training data set that belong to pathological subjects and ERNN4 is trained utilizing those exemplars in the training data set that belong to PD or HD diseases.

On successful completion of training, each modular ERNN is tested independently. ERNN1 is tested utilizing the entire testing data set, each of ERNN2 and ERNN3 is tested utilizing those exemplars in the testing data set that belong to pathological subjects and ERNN4 is tested utilizing PD and HD subjects from the testing database only. Tables 2–5 present the performance results for each ERNN separately. Here each

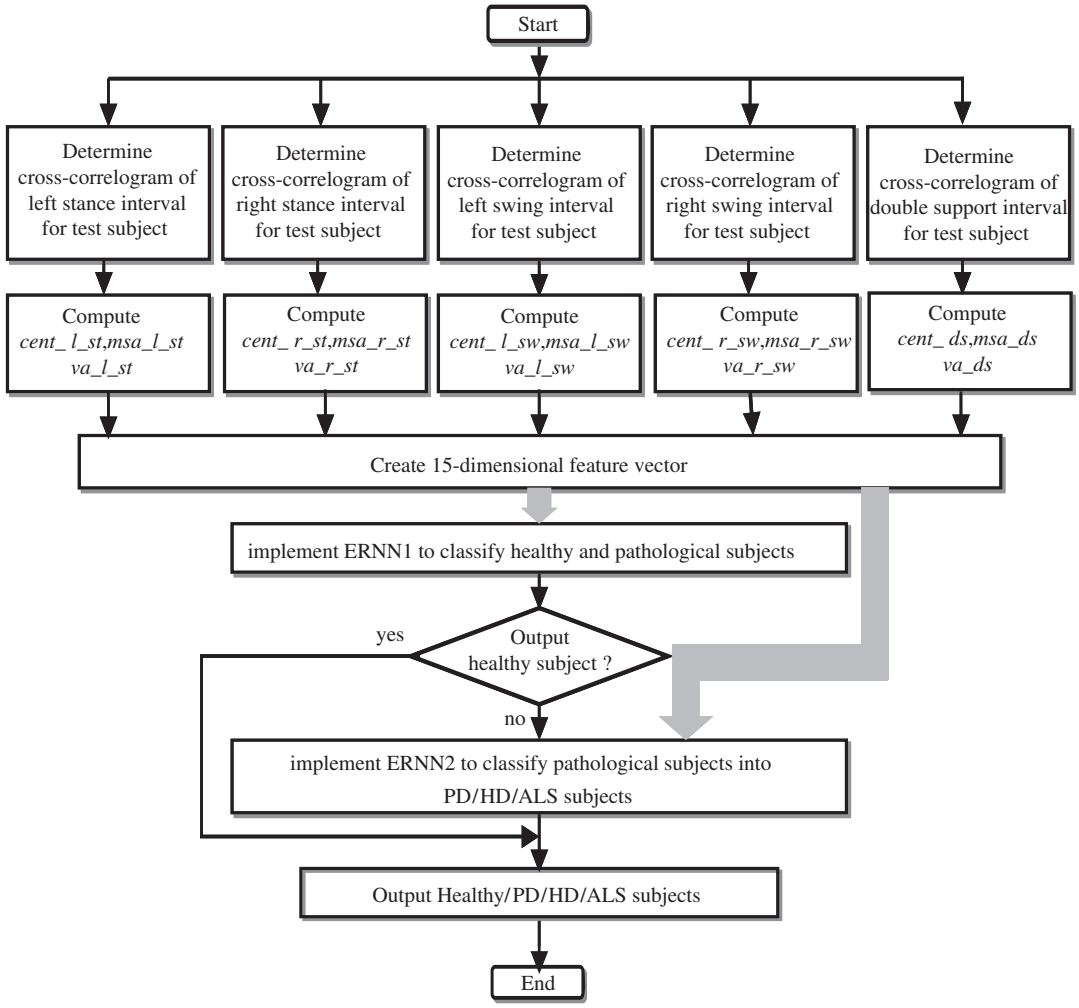

Figure 7: *Flowchart representation of scheme 1.*

ERNN was implemented 20 times and the percent classification results are mentioned in each case with the corresponding mean, standard deviation and range of results obtained employing 20 such runs for each ERNN. Each system was also implemented in accordance with N-crossfold validation theory with $N = 2$, i.e. the whole set of experiments was carried out a second time by swapping the composite training and testing data sets and the result of a particular run is considered as the mean of the two runs conducted by swapping training and testing data sets.

From Tables 2–5 it can be seen that, whenever the proposed cross-correlation aided modular ERNNs are implemented for binary classification purposes, they can comfortably attain 90.0% or more classification accuracy: ERNN1 reported a mean of 90.6%, ERNN3 reported as high as 97.8% and ERNN4 reported 94.1% accuracy. For ERNN2, which employed a three-class classification algorithm, accuracy was understandably a little lower, i.e. 89.8%. For each of them, the performance is compared by utilizing fuzzy c-means (FCM) clustering (Abonyi *et al.*, 2006), Gustafson–Kessel (GK) fuzzy clustering (Abonyi *et al.*, 2006) and BPNN based (Demuth & Beale, 1998) classification algorithms. Each of these classification/clustering

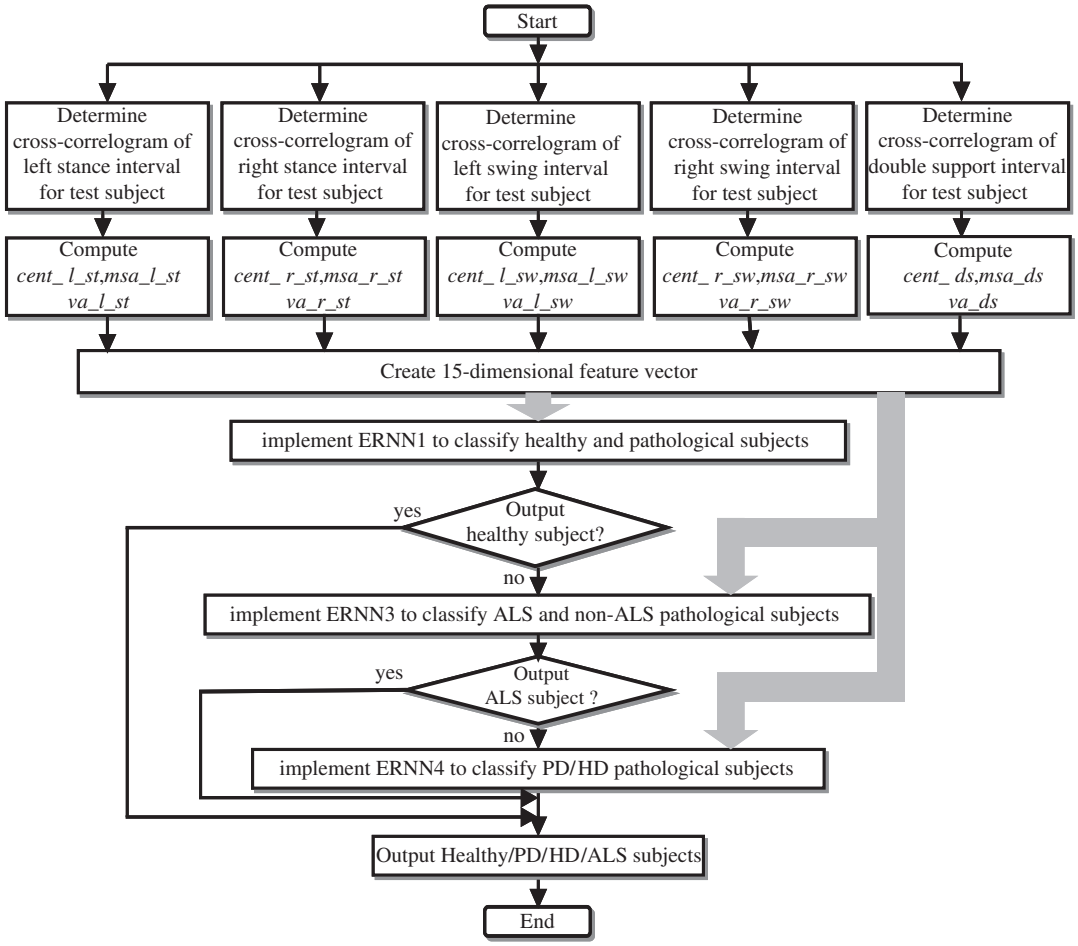

Figure 8: *Flowchart representation of scheme 2.*

Table 2: *Classification performance of ERNN1*

Algorithm	*Classification accuracy*								
	Healthy subject			*Pathological subject*			*Overall*		
	Mean (%)	*Std dev. (%)*	*Range (%)*	*Mean (%)*	*Std dev. (%)*	*Range (%)*	*Mean (%)*	*Std dev. (%)*	*Range (%)*
FCM clustering	93.3	–	–	55.3	–	–	64.5	–	–
GK fuzzy clustering	80.0	–	–	55.3	–	–	61.3	–	–
BPNN	61.5	9.9	50.0–75.0	88.4	2.8	82.6–91.3	81.2	2.7	77.4–83.9
ERNN1	90.0	5.1	87.5–100	90.9	3.1	87.1–93.6	90.6	1.8	87.1–93.6

Note: Each fuzzy clustering result is reported on a single-run basis and hence no standard deviation and range values of percent classification accuracies are mentioned.

Table 3: *Classification performance of ERNN2*

Algorithm	*Classification accuracy*											
	ALS			*PD*			*HD*			*Overall*		
	Mean (%)	*Std dev. (%)*	*Range (%)*	*Mean (%)*	*Std dev. (%)*	*Range (%)*	*Mean (%)*	*Std dev. (%)*	*Range (%)*	*Mean (%)*	*Std dev. (%)*	*Range (%)*
FCM clustering	61.5	–	–	60.0	–	–	37.0	–	–	51.0	–	–
GK fuzzy clustering	30.7	–	–	86.7	–	–	10.5	–	–	38.3	–	–
BPNN	25.0	8.7	16.7–33.0	63.8	3.9	62.5–75.0	60.0	5.8	55.5–66.7	52.1	2.9	47.8–56.5
ERNN2	89.1	8.2	83.3–100	80.0	7.5	75.0–100	97.2	4.9	88.9–100	89.8	3.2	87.0

Note: Each fuzzy clustering result is reported on a single-run basis and hence no standard deviation and range values of percent classification accuracies are mentioned.

Table 4: *Classification performance of ERNN3*

Algorithm	*Classification accuracy*								
	ALS			*Non-ALS*			*Overall*		
	Mean (%)	*Std dev. (%)*	*Range (%)*	*Mean (%)*	*Std dev. (%)*	*Range (%)*	*Mean (%)*	*Std dev. (%)*	*Range (%)*
FCM clustering	92.3	–	–	55.8	–	–	66.0	–	–
GK fuzzy clustering	84.6	–	–	44.0	–	–	55.3	–	–
BPNN	50.0	0.0	50.0–50.0	83.5	5.4	76.5–88.7	74.8	4.0	69.6–78.3
ERNN3	91.7	8.6	83.3–100	99.4	1.8	94.1–100	97.8	2.6	91.3–100

Note: Each fuzzy clustering result is reported on a single-run basis and hence no standard deviation and range values of percent classification accuracies are mentioned.

Table 5: *Classification performance of ERNN4*

Algorithm	*Classification accuracy*								
	PD			*HD*			*Overall*		
	Mean (%)	*Std dev. (%)*	*Range (%)*	*Mean (%)*	*Std dev. (%)*	*Range (%)*	*Mean (%)*	*Std dev. (%)*	*Range (%)*
FCM clustering	93.3	–	–	55.3	–	–	64.5	–	–
GK fuzzy clustering	80.0	–	–	55.3	–	–	61.3	–	–
BPNN	51.3	13.7	37.5–75.0	68.9	6.8	56.6–77.7	60.6	5.6	53.0–70.6
ERNN4	87.5	4.1	75.0–100	99.4	2.5	88.9–100	93.8	1.3	88.2–94.1

Note: Each fuzzy clustering result is reported on a single-run basis and hence no standard deviation and range values of percent classification accuracies are mentioned.

algorithms is initiated by the identical cross-correlation-based feature extraction procedure described earlier and hence all of them are based on 15-dimensional feature vectors. Each fuzzy clustering result is reported on a single-run basis. However, as BPNNs, like ERNNs, also employ supervised neural network based training procedures, they are employed in an identi-

Table 6: *Composite classification performance for scheme 1 and scheme 2*

Scheme	*ALS (%)*	*PD (%)*	*HD (%)*	*Healthy subject (%)*	*Overall (%)*
Scheme 1	83.3	83.3	78.0	87.5	83.8
Scheme 2	83.3	87.5	88.9	87.5	87.1

cal manner to ERNNs. Hence each BPNN result is reported on the basis of 20 runs, with their corresponding mean, standard deviation and range values. Each fuzzy clustering algorithm is implemented for the complete database, i.e. utilizing 100% of the exemplars in each data set. In each case, it can easily be seen that the performance of ERNN based systems is much superior compared to other competing algorithms. While fuzzy clustering based unsupervised procedures consistently produced worst results with classification accuracy varying in the range 51%–66%, the BPNN based supervised procedure produced inferior results with mean classification accuracy in the range 52.1%–81.2%. For fuzzy clustering schemes, a variation of the fuzzy exponent m in the range [1.1, 3.0] could not improve the result. Once these encouraging results were obtained with each modular ERNN, we employed the composite hierarchical schemes, scheme 1 and scheme 2, to obtain the automated gait identification tools as a four-class classification system. Table 6 reports these results which show that scheme 1 could produce 83.8% and scheme 2 could produce 87.1% overall accuracy. These results of scheme 1 and scheme 2 are reported with the best performing modular ERNNs, taken as their building blocks. These accuracies are a little less than individual accuracies of modular ERNNs, when implemented in standalone form. But this is understandable as each composite scheme employs two or three modular ERNNs, in hierarchical form. Tables 7 and 8 present the confusion matrices corresponding to the scheme 1 and scheme 2 results, respectively, presented in Table 6.

To have a realistic understanding of how strong or weak the proposed schemes are, we can compare these results with some of the other results reported utilizing gait signals. Our schemes are based on signals acquired from 63 subjects and results are reported on the basis of 62 subjects (as one subject is taken as the reference subject). In Giles *et al.* (1990), the SVM based procedure could solve the binary classification problem into young/elderly gaits, utilizing 24 statistical features extracted from minimum foot clearance data of 58 patients, with a mean classification accuracy of 83.3%. Compared to their scheme, each of our binary classification modular ERNN systems could comfortably produce more than 90% accuracy results and with fewer input features (i.e. 15). In Begg *et al.* (2005), even after the introduction of a hill-climbing algorithm for relevant feature selection (which introduces significant additional computational burden) the binary classification result could not improve more than 90%. In Barton and Lees (1997), another neural network based gait classification scheme was proposed using features from hip–knee joint angle measures. The problem was configured as a three-class classification problem and they

Table 7: *Confusion matrix for scheme 1*

Actual class	*Predicted class*			
	ALS	*PD*	*HD*	*Healthy*
ALS	5	0	1	0
PD	0	7	1	0
HD	0	1	7	1
Healthy	0	0	1	7

Table 8: *Confusion matrix for scheme 2*

Actual class	*Predicted class*			
	ALS	*PD*	*HD*	*Healthy*
ALS	5	1	0	0
PD	1	7	0	0
HD	0	0	8	1
Healthy	0	0	1	7

utilized data from eight subjects only. This scheme reported a classification ratio of 83.3% only. In the light of these discussions, our modular ERNNs reporting 90.3%–98.5% classification accuracy for binary classification jobs, 87.0% accuracy for three-class classification jobs and an accuracy as high as 87.1% for the composite scheme, considering the complete problem as a four-class classification problem, should be considered as very promising and encourage solutions for analysing gait signals to segregate healthy subjects from pathological subjects and to identify the source of the neurological disorder in pathological subjects.

6. Conclusion

In this work an attempt has been made to develop a robust algorithm which can automatically identify healthy/pathological gait and the type of neurological disease. Cross-correlation has been proposed as a formidable feature extraction tool and the ERNN has been effectively employed as an automated gait pattern classifier utilizing these extracted features.

Two gait identification schemes have been proposed here, utilizing several modular ERNNs in hierarchical form. Each of these schemes has been successfully implemented as a multiclass classification tool where one can segregate the input gait signals pertaining to healthy subjects and pathological subjects suffering from specific neurological disorders, i.e. PD, HD and ALS. The performances of the proposed schemes have been evaluated by considering some benchmark signals and very encouraging results have been reported compared with other contemporary algorithms available in practice.

The proposed methods show how modular RNNs can be effectively utilized for the specific problem under consideration and we utilized Elman's version of RNN to develop these modular neural networks. This will encourage us to make an in-depth study of the feasibility of implementing several candidate RNN algorithms available in the literature (e.g. Jordan's network, Pollack's network, finite impulse response networks, Laguerre models etc.) and to compare their performance. We intend to undertake this study as a future extension of the current work.

References

ABONYI, J., B. BALASKO and B. FEIL (2006) *Fuzzy Clustering and Data Analysis Toolbox*, available at http://www.fmt.vein.hu/softcomp/software.html.

BARIŞÇI, N. and F. HARDALAÇ (2007) Application of an adaptive neuro-fuzzy inference system for classification of Behcet disease using the fast Fourier transform method, *Expert Systems*, **24** (2), 123–130.

BARTON, J.G. and A. LEES (1997) An application of neural networks for distinguishing gait patterns on the basis of hip–knee joint angle diagrams, *Gait Posture*, **5**, 28–33.

BEGG, R.K., M. PALANISWAMI and B. OWEN (2005) Support vector machines for automated gait classification, *IEEE Transactions on Biomedical Engineering*, **52** (5), 828–838.

BOSE, N.K. and P. LIANG (1998) *Neural Network Fundamentals with Graphs, Algorithms and Applications*, New Delhi: Tata McGraw-Hill.

BRACEWELL, R.N. (2000) *The Fourier Transform and its Applications*, 3rd edn, Maidenhead: McGraw-Hill.

CARLETTI, T., D. FANELLI and A. GUARINO (2006) A new route to non invasive diagnosis in neurodegenerative diseases?, *Neuroscience Letters*, **394**, 252–255.

DAVIS, R.B. III (1988) Clinical gait analysis, *IEEE Engineering in Medicine and Biology Magazine*, September, 35–40.

DELGADO, M., M.C. PEGALAJAR and M.P. CUÉLLAR (2006) Memetic evolutionary training for recurrent neural networks: an application to time-series prediction, *Expert Systems*, **23** (2), 99–115.

DEMUTH, H. and M. BEALE (1998) *Neural Network Toolbox For Use with MATLAB*, Version 3, Natwick MA: The Mathworks.

DURBIN, B., S. DUDOIT and M.J. VAN DER LAAN (2008) A deletion/substitution/addition algorithm for classification neural networks, with applications to biomedical data, *Journal of Statistical Planning and Inference*, **138** (2), 464–488.

FILDES, B. (1994) *Injuries Among Older People: Falls at Home and Pedestrian Accidents*, Melbourne, FL: Dove Publications.

GILES, C.L., G. SUN, H.H. CHEN, Y.C. LEE and D. CHEN (1990) Higher order recurrent network and grammatical inference, *Advances in Neural Information Processing Systems*, **2**, 380–387.

GÜLER, İ. and E.D. ÜBEYLI (2005) An expert system for detection of electrocardiographic changes in patients with partial epilepsy using wavelet-based neural networks, *Expert Systems*, **22** (2), 62–71.
GÜLER, İ. and E.D. ÜBEYLI (2006) Combined neural network model to compute wavelet coefficients, *Expert Systems*, **23** (3), 159–173.
HAYKIN, S. (2004) *Neural Networks: A Comprehensive Foundation*, New Delhi: Pearson Education, Sixth Indian Reprint.
HOLZREITER, S.H. and M.E. KOHLE (1993) Assessment of gait pattern using neural networks, *Journal of Biomechanics*, **26**, 645–651.
IFEACHER, E.C. and B.W. JERVIS (2001) *Digital Signal Processing – A Practical Approach*, 2nd edn, Upper Saddle River, NJ: Prentice Hall, Pearson Education.
JORDON, M. (1986) Serial order: a parallel distributed processing approach, *ICS Rep. 8604*, Institute of Cognitive Science, University of California at San Diego.
KUPPUSAMY, K., W. LIN and E.M. HAACKE (1997) Statistical assessment of crosscorrelation and variance methods and the importance of electrocardiogram gating in functional magnetic resonance imaging, *Magnetic Resonance Imaging*, **15** (2), 169–181.
LEE, S.-W. and H.-H. SONG (1997) A new recurrent neural network architecture for visual pattern recognition, *IEEE Transactions on Neural Networks*, **8** (2), 331–340.
MIZUNO-MATSUMOTO, Y., G.K. MOTAMEDI, W.R.S. WEBBER and R.P. LESSER (2002) Wavelet-crosscorrelation analysis can help predict whether bursts of pulse stimulation will terminate after discharges, *Clinical Neurophysiology*, **113** (1), 33–42.
MIZUNO-MATSUMOTO, Y., G.K. MOTAMEDI, W.R.S. WEBBER, R. ISHII, S. UKAI, T. KAISHIMA, K. SHINOSAKI and R.P. LESSER (2005) Wavelet-crosscorrelation analysis of electrocorticography recordings from epilepsy, *International Congress Series*, Amsterdam: Elsevier Science, Vol. 1278, pp., 411–414.
NIGG, B.M., V. FISHER and J.L. RONSKY (1994) Gait characteristics as a function of age and gender, *Gait Posture*, **2**, pp., 213–220.
OSTROSKY, K.M., J.M. VANSWEARINGEN, R.G. BURDETT and Z. GEE (1994) A comparison of gait characteristics in young and old subjects, *Physical Therapy*, **74**, 637–646.
PIZZI, N.J. (2001) Bleeding predisposition assessments in tonsillectomy/adenoidectomy patients using fuzzy interquartile encoded neural networks, *Artificial Intelligence in Medicine*, **21** (1–3), 65–90.
POLLACK, J.B. (1991) The induction of dynamical recognizers, *Machine Learning*, **7**, 227–252.
ROBERTS, M.J. (2003) *Signals and Systems – Analysis using Transform Methods and MATLAB*, New Delhi: Tata McGraw-Hill.
SULJAGIC, S., N. RAJSIC, J. IVANUS, Z. BOZOVIC, A. KALAUZI, D. RAPAJIC and G. NEDOVIC (1996) The predictive role of *t*-histograms of crosscorrelation *R*-coefficients in the analysis of ictal EEG activity, *Electroencephalography and Clinical Neurophysiology*, **99** (4), 320.
SÜT, N. and M. ŞENOCAK (2007) Assessment of the performances of multilayer perceptron neural networks in comparison with recurrent neural networks and two statistical methods for diagnosing coronary artery disease, *Expert Systems*, **24** (3), 131–142.
ÜBEYLI, E.D. (2007) Comparison of different classification algorithms in clinical decision-making, *Expert Systems*, **24** (1), 17–31.
WINTER, D. (1991) *The Biomechanics and Motor Control of Human Gait: Normal, Elderly, and Pathological*, Waterloo, ON: University of Waterloo Press.
ZHOU, S.M. and L.D. XU (1999) Dynamic recurrent neural networks for a hybrid intelligent decision support system for the metallurgical industry, *Expert Systems*, **16** (4), 240–247.

The authors

Saibal Dutta

Saibal Dutta received the BE and ME degrees in electrical engineering from Jadavpur University, Kolkata, India, in 1999 and 2002, respectively. Currently, he is a senior lecturer in the Department of Electrical Engineering, Heritage Institute of Technology, Kolkata. His research interests include signal processing, neural networks and smart instrumentation.

Amitava Chatterjee

Amitava Chatterjee received the BE, ME and PhD degrees in electrical engineering from Jadavpur University, Kolkata, India, in 1991, 1994 and 2002, respectively. In 1997, he joined the Department of Electrical Engineering, Jadavpur University, as a faculty member, where he is presently serving as a Reader. In 2003, he received the Japanese Government (Monbukagakusho) Scholarship

and went to Saga University, Saga, Japan. In early 2004, he was invited as a Teacher-Researcher in the University of Paris XII, Val de Marne, France. From November 2004 to November 2005, he was with the University of Electro-Communications, Tokyo, Japan, on a JSPS Postdoctoral Fellowship for Foreign Researchers. His research interests include intelligent instrumentation and control, signal processing, image processing and robotics. He has published more than 55 technical papers, including 32 international journal papers, in his areas of research interest.

Sugata Munshi

Sugata Munshi obtained the BEE and MEE degrees from Jadavpur University, Kolkata, India, in 1980 and 1985, respectively. He worked as an engineer in the Plasma Physics Division of Saha Institute of Nuclear Physics, India, from 1985 to 1990. In 1986, he had training on the 'Tokamak' machine in the Heavy Engineering Works of Toshiba Corporation in Japan. In 1990 he joined the Electrical Engineering Department of Jadavpur University as a faculty member. At present, he is a Reader in this department. He has published about 30 research papers in refereed journals and about 20 papers in conference proceedings. He was the joint recipient of The President of India's Prize (English) in 1989–90, the Pandit Madan Mohan Malaviya Memorial Prize in 1989–90, the Sir Thomas Ward Memorial Prize in 1994–95, the Tata Rao Medal, awarded by the Institution of Engineers (India), in 1996–97 and a Certificate of Merit from IE (India) in 1996–97. His current fields of interest are signal processing, surge phenomena in power equipment and sensor systems.